Stanford Exploration Project, Report 110, September 18, 2001, pages 1–62

Stolt residual migration for converted waves

Daniel Rosales, Paul Sava, and Biondo Biondi [1]

ABSTRACT

PS velocity analysis is a new frontier in converted-waves seismic imaging. To obtain one consistent image, it is necessary to estimate correctly both the P-waves velocity model and the S-waves velocity model. Stolt residual migration is a useful technique for image update and velocity analysis. This paper extends Stolt prestack residual migration in order to handle two different velocity fields. The operator that we introduce is promising for PS velocity analysis. We present a theoretical discussion of our new operator, and discuss its ability to focus PS images.

INTRODUCTION

Stolt residual prestack migration is a useful tool to improve the quality of the image and to perform migration velocity analysis (Stolt, 1996; Sava, 1999, 2000). To update a PS image, we extend Stolt prestack residual migration for two different velocity fields.

The extension of Stolt residual migration for converted waves can be done in two ways. An approximate method uses two different residual velocities in each of the two square roots of the double square root equation. The exact method calculates an appropriate transformation kernel that is able to handle both velocity fields. We will discuss both ways in the theory part. Moreover, we present synthetic examples, with both constant velocity and depth variant velocity models. For constant velocity, we show that we are able to focus the image after a migration with wrong velocities. For depth-variant velocity, we show that we are able to improve the image.

THEORY

Stolt (1996) first introduced prestack residual migration. Sava (1999) reformulated Stolt residual migration in order to handle prestack depth images. This section presents the extension of Sava (1999) for two different wavefields, therefore, two different velocities. We present this extension for converted waves data, where the P to S conversion occurs at the reflector. Although the formulation involves P-velocities and S-velocities, its application is not limited to converted waves only. Rosales and Biondi (2001) present a possible application for imaging under salt edges.

[1] **email:** daniel@sep.stanford.edu,paul@sep.stanford.edu,biondo@sep.stanford.edu

Residual prestack Stolt migration operates in the Fourier domain. Considering the representation of the input data in shot-geophone coordinates, the mapping from the data space to the model space takes the form

$$k_z = \frac{1}{2}\left(\sqrt{\frac{\omega^2}{v_p^2} - k_s^2} + \sqrt{\frac{\omega^2}{v_s^2} - k_g^2}\right), \tag{1}$$

where k_s, k_g, v_p, and v_s stand for, respectively, the source and geophone wavenumbers, and the P and S velocities.

In residual prestack Stolt migration for converted waves, we attempt to simultaneously correct the effects of migrating with two inaccurate velocity fields.

Supposing that the initial migration was done with the velocities v_{0p} and v_{0s}, and that the correct velocities are v_{mp} and v_{ms}, we can then write

$$\begin{cases} k_{z_0} = \frac{1}{2}\left(\sqrt{\frac{\omega^2}{v_{0p}^2} - k_s^2} + \sqrt{\frac{\omega^2}{v_{0s}^2} - k_g^2}\right) \\ k_{z_m} = \frac{1}{2}\left(\sqrt{\frac{\omega^2}{v_{mp}^2} - k_s^2} + \sqrt{\frac{\omega^2}{v_{ms}^2} - k_g^2}\right). \end{cases} \tag{2}$$

Solving for ω^2 in the first equation of (2) and substituting it in the second equation of (2), we obtain the expression for prestack Stolt depth residual migration for converted waves [equations (3) and/or (4)] (see Appendix A, for details in derivation)

$$k_{z_m} = \tfrac{1}{2}\sqrt{\rho_p^2\overline{\overline{\kappa_0{}^2}} - k_s^2} + \tfrac{1}{2}\sqrt{\rho_s^2\gamma_0{}^2\overline{\overline{\kappa_0{}^2}} - k_g^2}, \tag{3}$$

$$k_{z_m} = \tfrac{1}{2}\sqrt{\rho_p^2\overline{\overline{\kappa_0{}^2}} - k_s^2} + \tfrac{1}{2}\sqrt{\rho_p^2\gamma_m{}^2\overline{\overline{\kappa_0{}^2}} - k_g^2}, \tag{4}$$

where $\overline{\overline{\kappa_0{}^2}}$ is the transformation kernel and is defined as

$$\overline{\overline{\kappa_0{}^2}} = \frac{4(\gamma_0{}^2+1)k_{z_0}{}^2 + (\gamma_0{}^2-1)(k_g{}^2 - k_s{}^2) - 4k_{z_0}\sqrt{(1-\gamma_0{}^2)(\gamma_0{}^2 k_s{}^2 - k_g{}^2) + 4\gamma_0{}^2 k_{z_0}{}^2}}{(\gamma_0{}^2-1)^2},$$

and $\rho_p = \frac{v_{0p}}{v_{mp}}$, $\rho_s = \frac{v_{0s}}{v_{ms}}$, and $\gamma = \frac{v_p}{v_s}$.

In equation (2) it appears that Stolt residual migration for converted waves depends on four parameters: v_{0p}, v_{0s}, v_{mp}, v_{ms}. These four degrees of freedom can be reduced to three (ρ_p, ρ_s and γ), as seen in equations (3) and (4) and demonstrated in Appendix A. This is important, because a three parameters search for updating converted waves images is simpler than a four parameters search. However, it would be useful to further reduce the number of parameter to two. Assuming that the v_p/v_s ratio is the same after and before the residual migration process, it is possible to simplify equations (3) and/or (4) into a two parameter equation:

$$k_{z_m} = \tfrac{1}{2}\sqrt{\rho_p^2\overline{\kappa_0{}^2} - k_s^2} + \tfrac{1}{2}\sqrt{\rho_p^2\gamma^2\overline{\kappa_0{}^2} - k_g^2}, \tag{5}$$

where the transformation kernel takes the form

$$\overline{\kappa_0{}^2} = \frac{4(\gamma^2+1){k_{z_0}}^2 + (\gamma^2-1)({k_g}^2 - {k_s}^2) - 4k_{z_0}\sqrt{(1-\gamma^2)(\gamma^2{k_s}^2 - {k_g}^2) + 4\gamma^2{k_{z_0}}^2}}{(\gamma^2-1)^2}.$$

If we just specify two different ratios in both square roots of Sava's (1999) formulation we have

$$k_{z_m} = \tfrac{1}{2}\sqrt{\rho_p^2\kappa_0^2 - k_s^2} + \tfrac{1}{2}\sqrt{\rho_s^2\kappa_0^2 - k_g^2}, \tag{6}$$

where the transformation kernel has the same form as the one of PP waves:

$$\kappa_0^2 = \frac{\left[4k_{z_0}^2 + (k_g - k_s)^2\right]\left[4k_{z_0}^2 + (k_g + k_s)^2\right]}{16k_{z_0}^2}.$$

Equation (6) shows another way of doing prestack residual migration for converted waves. Although equations (5) and (6) may look similar because they depend on only two parameters, the transformation kernels (κ_0 and $\overline{\kappa_0}$) are different. Equation (6) has a similar transformation kernel as the conventional PP prestack residual migration, while equation (5) presents a kernel deduced for the case of converted waves.

It is important to note that all three equations (3), (5), and (6) reduce to the same expressions in the limit when of v_s tends to v_p, or γ tends to 1. All of them reduce to the simple case of prestack residual migration for conventional PP data. Appendix B demonstrates this result.

NUMERICAL EXAMPLES

Impulse Responses

Figure 1 shows the impulse response of the three residual prestack migration operators [equations (3), (5), (6)].

Figure 1a presents the impulse response for equation (3), with $\rho_p = 1.2$, $\rho_s = 1.2$ and $\gamma_0 = 2$. Figure 1b presents the impulse response for equation (5), with $\rho_p = 1.2$ and $\gamma = 2$. As expected from the theory discussed in the previous section, Figure 1a and Figure 1b are identical because $\gamma = \gamma_0$.

Figure 1c presents the impulse response for equation (6), with $\rho_p = 1.2$, $\rho_s = 1.2$. It is possible to observe the difference with respect to figures 1a and 1b. The difference is due to the approximation in the transformation kernel.

Figure 2 demonstrates the differences between equations (3) and (5). Figure 2a shows the impulse response for equation (3) with, $\rho_p = 0.9$, $\rho_s = 1.4$ and $\gamma_0 = 2$. Figure 2b shows the impulse response for equation (5) with, $\rho_p = 0.9$ and $\gamma = 2$. It is easy to observe the difference between the impulse responses due to the approximation in the transformation kernel.

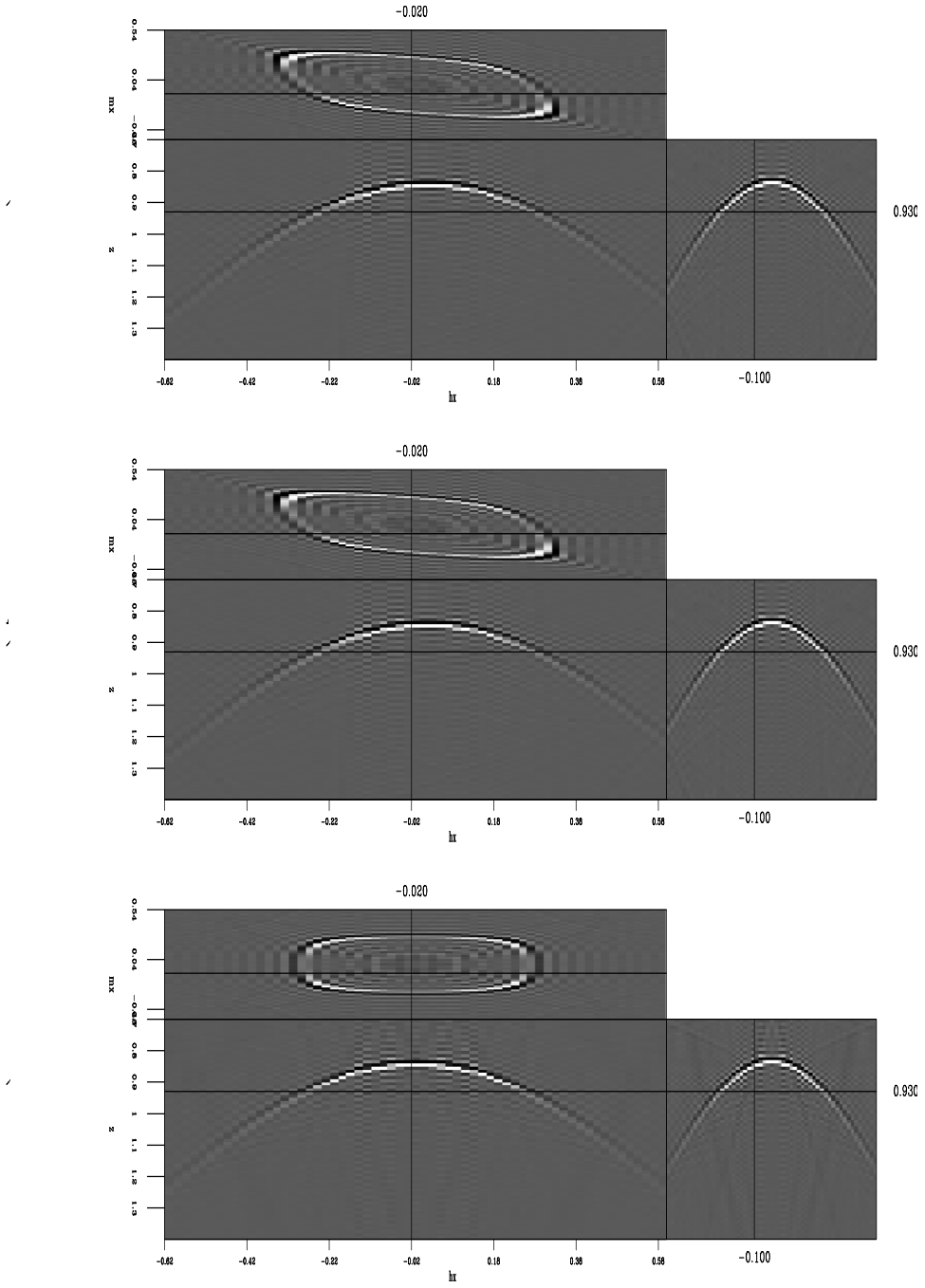

Figure 1: Impulse response for the residual prestack migration operators. From top to bottom, a) equation (3) for $\rho_p = 1.2$, $\rho_s = 1.2$, $\gamma_0 = 2$; b) equation (5) for $\rho_p = 1.2$, $\gamma = 2$; c) equation (6) for $\rho_p = 1.2$, $\rho_s = 1.2$. daniel1-imp [ER,M]

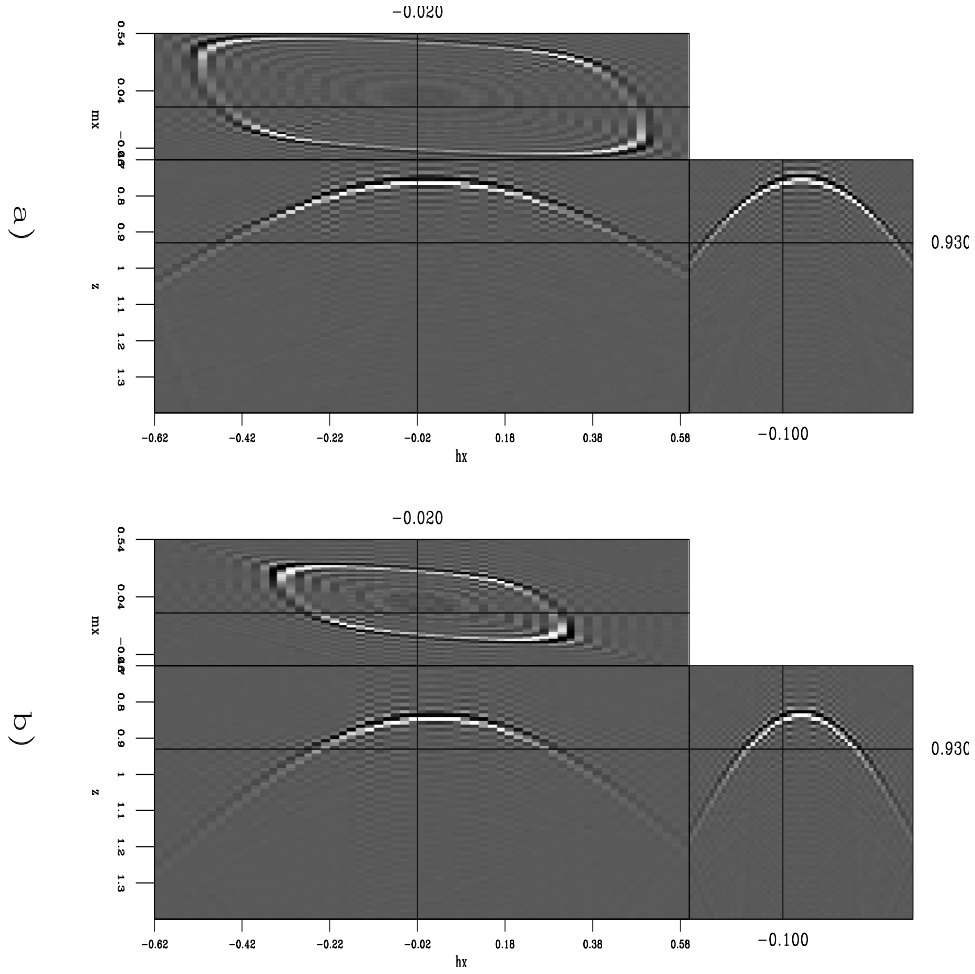

Figure 2: Impulse response for the residual prestack migration operators. From top to bottom, a) equation (3) for $\rho_p = 1.2$, $\rho_s = 1.4$, $\gamma_0 = 2$; b) equation (5) for $\rho_p = 1.2$, $\gamma = 2$. daniel1-imp2 [ER,M]

Residual migration with constant velocity

In order to test the accuracy of our operator we created a synthetic data set assuming a constant velocity model of $v_p = 3000$ m/s and $v_s = 1500$ m/s, and four reflectors having dips of 15°, 0°, −30°, −45°, respectively.

We first migrated the data with the wrong velocity, using shot-profile migration for converted waves (Rosales and Rickett, 2001), and extract angle-domain common-image gathers for converted waves (Rickett and Sava, 2001). We then applied Stolt residual prestack migration, using the methods described in the previous section.

We show the results of performing migration followed by residual prestack migration, when the initial migration was performed with the correct P-velocity, and with the S-velocity 15% too high. Figure 3 shows a comparison for the zero offset section, equivalent to the

stack final migrated section, of the residual migration result for equations (3), (5) and (6) and the migration with the correct velocity model. It is possible to observe that the result with the correct expression [equation(3)] produces an image similar to the image produced by the migration with the correct velocity. On the contrary, when we use the other two expressions we obtain poorly focused results.

Notice that because of the change in polarity between the negative and positive reflection angles, these zero-offset sections show degraded images. Rosales and Rickett (2001) discuss how to correct for the change in polarity. Therefore, we analyze the common image gathers. Figure 4 shows five common image gather all taken at the same surface location. From left to right: the good migration result, correction with the correct expression [equation (3)], correction with equation (5), correction with equation (6) and the bad migration result. It is possible to observe that the events after residual migration with the correct expression [equation (3)] are flat. Corrections with equations (5) and (6) yield to over and under corrected gathers, respectively.

Residual migration with vertical velocity gradient

Since Stolt residual prestack migration is based on the assumption of constant velocity, we will evaluate the accuracy for velocity models having depth dependence.

We create our second synthetic model using the same reflector geometry as the previous section and using a realistic depth velocity model of $v_{0p} = 1700$ m/s with a gradient of 0.15 s^{-1} and $v_{0s} = 300$ m/s with a gradient of 0.35 s^{-1},

As before, we perform the initial shot profile migration with a 15% positive perturbation in the S-velocity model. We perform residual migration with the RMS γ_0 value at approximately 1.5 km, and $\rho_p = 1$ and $\rho_s = 1.15$. Residual prestack migration could not recover the image correctly at all depths. However, we got a good approximation of it. Figures 5 and 6 show our results.

CONCLUSIONS

We introduced the extension of Stolt prestack residual migration for converted waves. Our new operator involves the selection of three parameters in order to update the image.

To help in the memory and disk space necessary for the implementation of our operator, we also derived approximations that reduce the number of free parameters to a two. The most appropriate way of reducing the number of parameters is by freezing one of them. Our experience suggests freezing γ_0 at the RMS value of the ratio between the P and the S migration velocities.

In constant velocity, we proved that we can recover the image obtained with an initial migration that uses an inaccurate velocity model. Therefore, we can update a migration with constant two-velocities model using our new operator. We can also update an image obtained

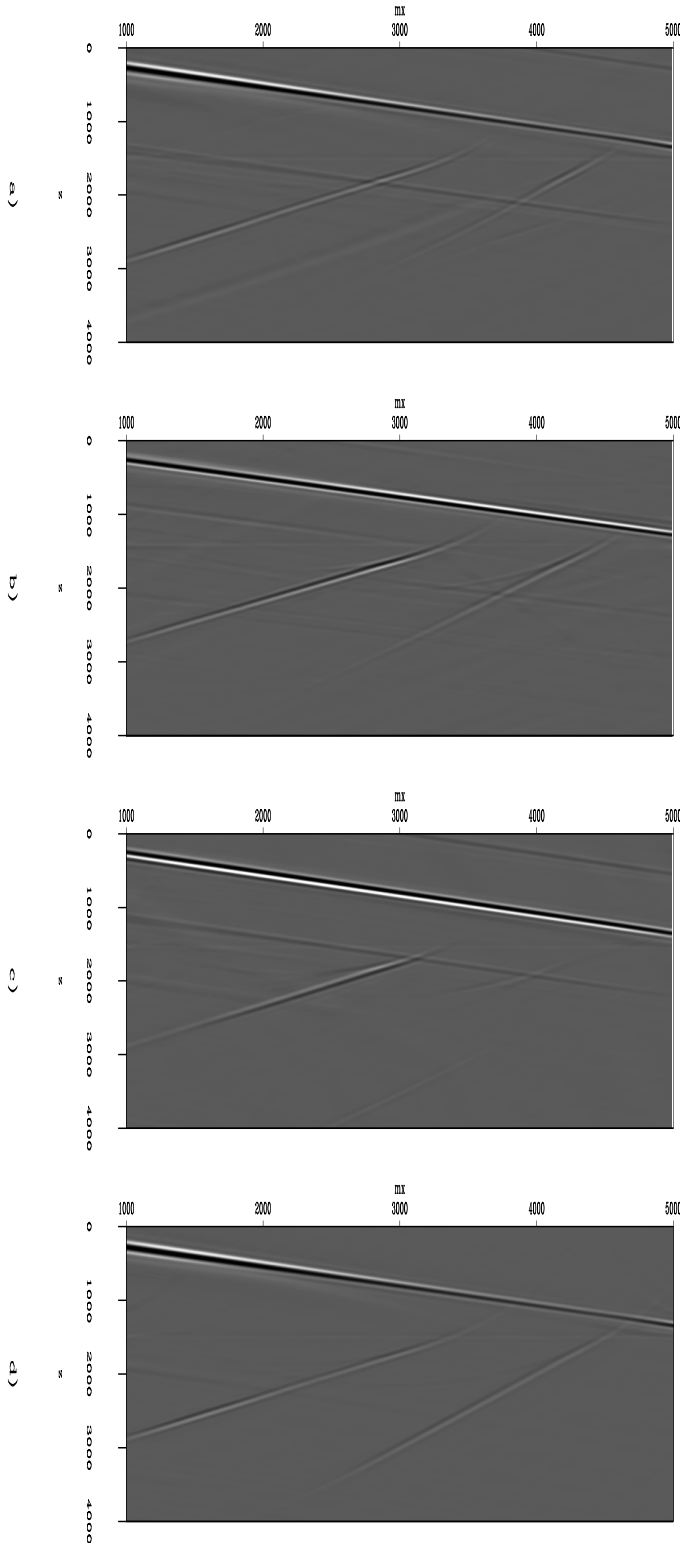

Figure 3: Zero offset section, equivalent to final migrated section, using the residual migration operator for: a) equation (3) for $\rho_p = 1$ $\rho_s = 1.15$, $\gamma_0 = 1.74$; b) equation (5) for $\rho_p = \rho_s = 1.15$ and $\gamma = 1.74$; c) equation (6) for $\rho_p = 1$ $\rho_s = 1.15$, d) migration with the correct velocity model. daniel1-cv1 [CR,M]

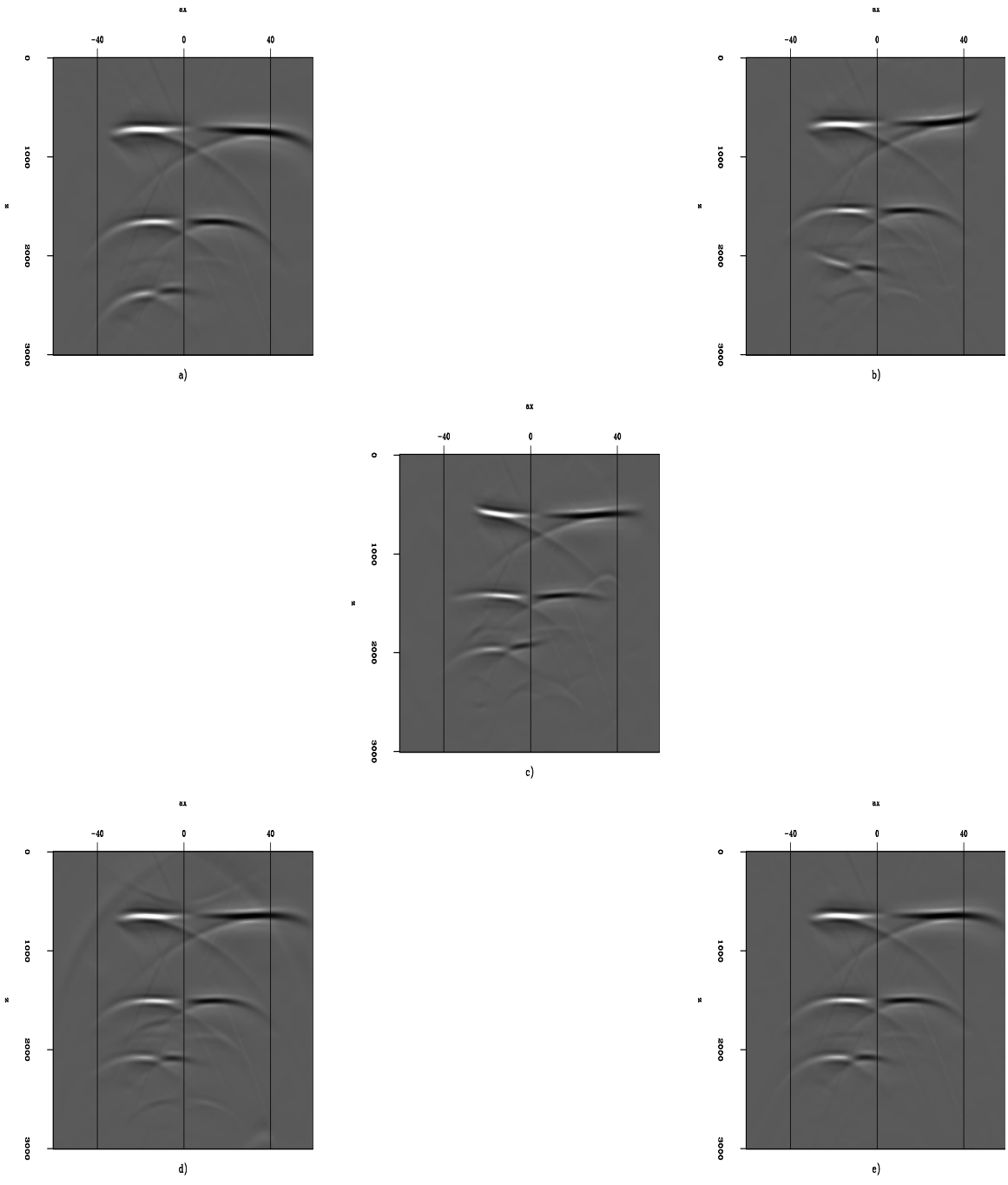

Figure 4: Angle domain common image gathers for, top to bottom and left to right: a) migration with 15% error in the *S*-velocity; b) residual migration with equation (6); c) residual migration with equation (5); d) residual migration with equation (3); e) migration with the correct velocity. daniel1-cv2 [CR,M]

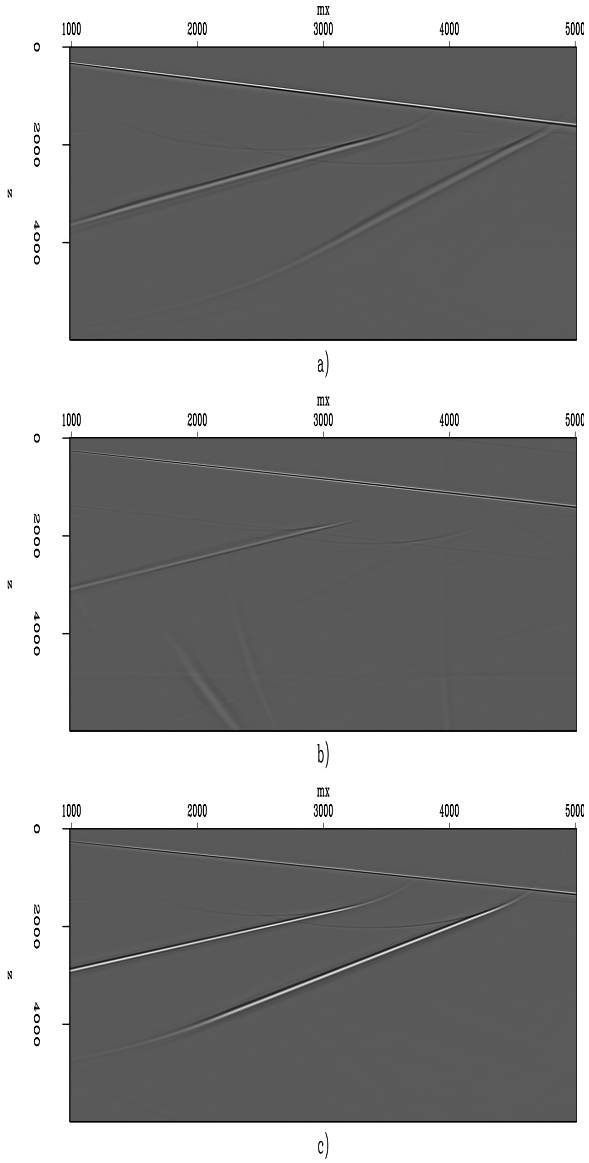

Figure 5: Zero offset section comparison, final migration stack, for: a) migration with 15% error in the *S*-velocity model; b) residual migration with equation (6) for $\rho_p = 1$, $\rho_s = 1.15$ and $\gamma_0 = 1.92$; c) migration with the correct velocity model. daniel1-vofz [CR,M]

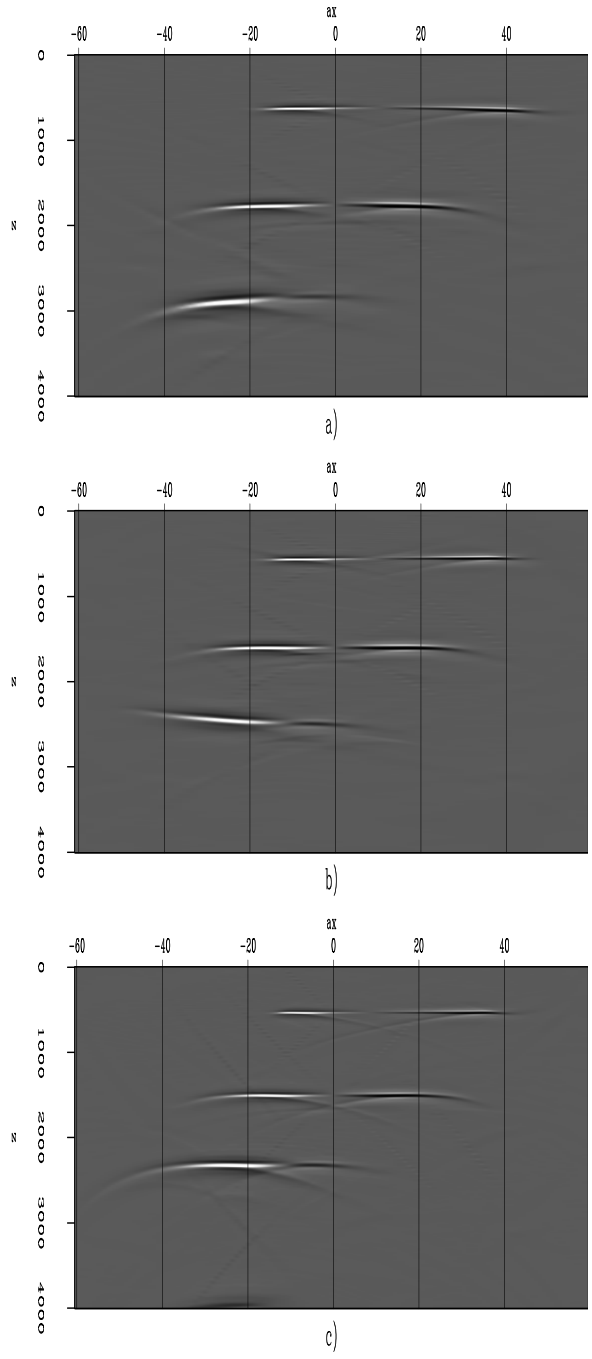

Figure 6: Zero offset section comparison, final migration stack, for: a) migration with 15% error in the S-velocity model; b) residual migration with equation (6) for $\rho_p = 1$, $\rho_s = 1.15$ and $\gamma_0 = 1.92$; c) migration with the correct velocity model. daniel1-vofz2 [CR,M]

with a depth variant velocity. However, the refocusing performed by residual migration is only approximate.

The advantages of having an operator to update converted waves images allow us to extrapolate our ability to handle multiple mode data. We hope that it will lead to more accurate methods for performing velocity analysis for converted waves.

APPENDIX A

Solving the first equation of:

$$\begin{cases} k_{z_0} = \frac{1}{2}\left(\sqrt{\omega^2 s_{p_0}^2 - k_s^2} + \sqrt{\omega^2 s_{s_0}^2 - k_g^2}\right) \\ k_{z_m} = \frac{1}{2}\left(\sqrt{\omega^2 s_{p_m}^2 - k_s^2} + \sqrt{\omega^2 s_{s_m}^2 - k_g^2}\right), \end{cases} \tag{A-1}$$

for ω^2 we have:

$$2k_z = \sqrt{\omega^2 s_{p_0}^2 - k_s^2} + \sqrt{\omega^2 s_{s_0}^2 - k_g^2},$$

and

$$\left(2k_z - \sqrt{\omega^2 s_{p_0}^2 - k_s^2}\right)^2 = \left(\sqrt{\omega^2 s_{s_0}^2 - k_g^2}\right)^2.$$

Squaring the previous equation and isolating the remaining square root we obtain:

$$4k_z^2 + \omega^2 s_{p_0}^2 - \omega^2 s_{s_0}^2 + k_g^2 - k_s^2 = 4k_z\sqrt{\omega^2 s_{p_0}^2 - k_s^2}.$$

Squaring the previous equations, grouping common terms, and setting equal to zero, we get:

$$\omega^4\left(s_{p_0}^2 - s_{s_0}^2\right)^2 + \omega^2\left[\left(8k_z^2 + 2k_g^2 - 2k_s^2\right)\left(s_{p_0}^2 - s_{s_0}^2\right) - 16k_z^2 s_{p_0}^2\right] + \left(4k_z^2 + k_g^2 - k_s^2\right)^2 + 16k_z^2 k_s^2 = 0.$$

Solving for ω^2 we obtain

$$\omega^2 = \frac{s_{s_0}^2\left(4k_z^2 + k_g^2 - k_s^2\right) + s_{p_0}^2\left(4k_z^2 + k_s^2 - k_g^2\right) \pm 4k_z^2\sqrt{s_{p_0}^2 s_{s_0}^2\left(4k_z^2 + k_g^2 + k_s^2\right) - s_{p_0}^4 k_g^2 - s_{s_0}^4 k_s^2}}{\left(s_{p_0}^2 - s_{s_0}^2\right)^2}. \tag{A-2}$$

We select the negative sign of the radical as the final solution for ω^2, as discussed in Appendix B.

Substituting the result of ω^2 in the second equation of relation (A-1), we obtain the relationship for residual prestack migration for converted waves.

In order to demonstrate this fact, we need to simplify the dispersion relation for ω^2 in terms of $\gamma_0 = \frac{v_{p_0}}{v_{s_0}}$, s_{p_0} and s_{s_0} depending on the source or receiver SSR equation.

$$\left(s_{p_0}^2 - s_{s_0}^2\right)^2 = s_{p_0}^4\left(1 - \gamma_0^2\right)^2$$

therefore,

$$\omega^2 = \frac{\gamma_0^2(A)+(B)-4k_z^2\sqrt{\gamma_0^2(C)-k_g^2-\gamma_0^4k_s^2}}{s_{p_0}^2\left(1-\gamma_0^2\right)^2},$$

since

$$k_{z_m} = \frac{1}{2}\left(\sqrt{\omega^2 s_{p_m}^2 - k_s^2}+\sqrt{\omega^2 s_{s_m}^2 - k_g^2}\right),$$

calling

$$\kappa_0^2 = \frac{\gamma_0^2 A + B - 4k_z^2\sqrt{\gamma_0^2 C - k_g^2 - \gamma_0^4 k_s^2}}{\left(1-\gamma_0^2\right)^2}, \tag{A-3}$$

we finally note that $\omega^2 = \frac{\kappa_0^2}{s_{p_0}^2}$. We then have equation (3), which is:

$$k_{z_m} = \frac{1}{2}\left(\sqrt{\gamma_0^2\rho_s^2\kappa_0^2 - k_g^2}+\sqrt{\rho_p^2\kappa_0^2 - k_s^2}\right). \tag{A-4}$$

APPENDIX B

We want to evaluate equations (3), (5) and (6) when $v_p = v_s$, or equivalently, when $\gamma_m = \gamma_0 = 1$.

It is possible to see from equation (A-3) that for the particular case of $\gamma_0 = 1$ we have a division by zero. Since we have a division by zero, we need to analyze the equation when we approach to $\gamma_0 \to 1$. For this purpose, we are going to use L'Hôpital. Therefore, we need to have a zero also in the numerator, which is possible for any value of k_z if, and only if, we choose the negative sign as a solution in equation (A-2).

Referring to equation (A-3) as $\kappa_0^2 = f(\gamma_0)/g(\gamma_0)$, and applying the L'Hôpital, we calculate the derivative with respect to γ_0 to $f(\gamma_0)$ and $g(\gamma_0)$.

We derive

$$\frac{\partial}{\partial\gamma_0} f(\gamma_0) = 2\gamma_0\left(4k_z^2+k_g^2-k_s^2\right) - 4k_z^2\frac{\gamma_0\left(8k_z^2+2k_g^2+2k_s^2-4\gamma_0^3k_s^2\right)}{\sqrt{\gamma_0^2\left(4k_z^2+k_g^2+k_s^2\right)-k_g^2-\gamma_0^4k_s^2}}.$$

On the other hand, the derivative of the denominator is:

$$\frac{\partial}{\partial\gamma_0}\left(\left(\gamma_0^2-1\right)^2\right) = 4\left(\gamma_0^2-1\right)\gamma_0.$$

Analyzing the limit for $\gamma_0 \to 1$ of the $f\prime(\gamma_0)/g\prime(\gamma_0)$, we still have a $\frac{0}{0}$ relation, which means we must re-apply L'Hôpital,

$$\frac{\partial}{\partial\gamma_0} f'(\gamma_0) = 2\left(4k_z^2+k_g^2-k_s^2\right) - \frac{k_z\gamma_0\left(8k_z^2+2k_g^2+2k_s^2-4\gamma_0^3k_s^2\right)^2}{\left(\gamma_0^2\left(4k_z^2+k_g^2+k_s^2\right)k_g^2-\gamma_0^4k_s^2\right)^{\frac{3}{2}}} + \frac{2k_z\left(8k_z^2+2k_g^2+2k_s^2-12\gamma_0^2k_s^2\right)}{\left(\gamma_0^2\left(4k_z^2+k_g^2+k_s^2\right)-k_g^2-\gamma_0^4k_s^2\right)^{\frac{1}{2}}}.$$

On the other hand, the second derivative of the denominator is:

$$\frac{\partial}{\partial \gamma_0} g'(\gamma_0) = 8\gamma_0^2.$$

We finally have

$$\lim_{\gamma_0 \to 1} \frac{f(\gamma_0)}{g(\gamma_0)} = \lim_{\gamma_0 \to 1} \frac{\frac{\partial}{\partial \gamma_0} f(\gamma_0)}{\frac{\partial}{\partial \gamma_0} g(\gamma_0)} = \lim_{\gamma_0 \to 1} \frac{\frac{\partial^2}{\partial \gamma_0^2} f(\gamma_0)}{\frac{\partial^2}{\partial \gamma_0^2} g(\gamma_0)}.$$

Therefore, we have κ_0^2 for $\gamma_0 \to 1$ reduces to:

$$\left[4k_z^2 + \left(k_g - k_s\right)^2\right]\left[4k_z^2 + \left(k_g + k_s\right)^2\right]$$

which is the expression for the conventional case of PP waves.

REFERENCES

Rickett, J., and Sava, P., 2001, Offset and angle domain common-image gathers for shot-profile migration: SEP–**108**, 27–34.

Rosales, D., and Biondi, B., 2001, On asymmetric Stolt residual migration for imaging under salt edges: SEP–**110**, 71–74.

Rosales, D., and Rickett, J., 2001, ps-wave polarity reversal in angle domain common-image gathers: SEP–**108**, 35–44.

Sava, P., 1999, Short note–on Stolt prestack residual migration: SEP–**100**, 151–158.

Sava, P., 2000, Variable-velocity prestack Stolt residual migration with application to a North Sea dataset: SEP–**103**, 147–157.

Stolt, R. H., 1996, Short note - a prestack residual time migration operator: Geophysics, **61**, no. 2, 605–607.